RESEARCH ARTICLE | MAY 01 2024

Experimental investigation of storm sewer geyser using a large-scale setup *⊙*

Special Collection: Flow and Civil Structures

Pratik Mahyawansi 🗷 💿 ; Sumit R. Zanje 💿 ; Abbas Sharifi 💿 ; Dwayne McDaniel 💿 ; Arturo S. Leon 💿



Physics of Fluids 36, 052101 (2024) https://doi.org/10.1063/5.0199012

A CHORUS





Articles You May Be Interested In

Modeling geysers triggered by an air pocket migrating with running water in a pipeline

Physics of Fluids (April 2023)

Flooding estimation under effects of future climate change using SWMM model in stormwater sewer system: Case study in Al-Samawa city

AIP Conf. Proc. (September 2023)

Air-water interaction in a partially filled circular pipe

Physics of Fluids (January 2025)



Physics of Fluids

Special Topics Open for Submissions

Learn More



Experimental investigation of storm sewer geyser using a large-scale setup

Cite as: Phys. Fluids **36**, 052101 (2024); doi: 10.1063/5.0199012

Submitted: 20 January 2024 · Accepted: 18 April 2024 ·

Published Online: 1 May 2024

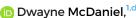
















AFFILIATIONS

¹Mechanical and Materials Engineering, Florida International University, Miami, Florida 33174, USA

Note: This paper is part of the special topic, Flow and Civil Structures.

- ^{a)}Author to whom correspondence should be addressed: pmahy002@fiu.edu
- b) Electronic mail: szanj001@fiu.edu
- c) Electronic mail: ashar092@fiu.edu
- d) Electronic mail: mcdaniel@fiu.edu
- e)Electronic mail: arleon@fiu.edu

ABSTRACT

The storm sewer geyser is a process where an air-water mixture violently erupts from a manhole. Despite the low hydrostatic pressure, violent eruptions can achieve a height of tens of meters above the ground. This current study experimentally investigates large-scale violent geysers using a large air pocket inserted from a pressurized air tank. The total length of the pipe system is approximately 88 m with a 0.1572 m diameter pipe. This large-scale experiment facilitates the investigation of spontaneous geyser eruptions. This study identifies the role of air-water volume ratio and coefficient of pressure (ratio of absolute initial static pressure to initial dynamic pressure) on the geyser intensity using eruption images and pressure plots. A total of 116 cases are tested, in which the volume ratio is parametrically increased from 0 to 1.1 under various operating conditions. A geyser score is defined to quantify the geyser eruption nature based on visual observations. The key findings are as follows: first, a sharp transition in geyser intensity is observed at the critical volume ratio of 0.5, and pre-transition and post-transition intensity exhibit a linear relationship with the volume ratio; and second, the critical volume ratio linearly varies with the coefficient of pressure.

Published under an exclusive license by AIP Publishing. https://doi.org/10.1063/5.0199012

I. INTRODUCTION

Storm sewer geysers are frequently observed in metropolitan cities such as Minneapolis, New York, and other major North American cities. In the event of heavy rainfall, the rapid pressurization of sewer lines can result in air entrapment, which can interact with the tunnel dropshaft (vertical pipe) and may produce a geyser. Figure 1 shows the critical stages of a storm sewer geyser, where an initially low water level in the tunnel is elevated by a large trapped air pocket similar to the Taylor bubble rise phenomenon. The force in the water rise can be strong enough to lift the metallic cover and spill sewer water on the road. Meanwhile, the air-water interface in the vertical pipe is atomized to form a mixed flow, which now moves at a faster speed and transforms the spillage into a violent geyser.

Recent climate change is resulting in an increasing trend of extreme precipitation. Additionally, for low-lying coastal cities, the gravity-driven sewer tunnels are subjected to elevated outlet pressure due to sea level rise.³ The elevated pressure reduces the effectiveness of

sewer tunnels and may result in an early transformation of stratified flow to pressurized flow, which can have large trapped air pockets. Recent studies have projected an increasing trend of relative sea level rises with 4.1 mm/year in the years 2040 to 2060. This means that the old sewer tunnels in coastal cities will be subjected to higher sea levels, potentially increasing the probability of tunnel pressurization, which can lead to geysers. In non-coastal cities, the old sewer tunnels may become overloaded due to the increasing trend of extreme precipitation. As a result, the city will receive more rainwater, potentially leading to frequent geysers and flooding. The violent eruptions can attain a height of 30 m as seen in some of the internet videos. These eruptions pose several safety hazards such as falling objects, flooding, and exposure to raw sewage and chemicals. Although the eruptions can be tens of meters high, the hydrostatic pressure head in the pipes is found to

The mechanism of these geysers is still an active research area, where our understanding of this problem has significantly been

 $^{^{2}}$ Civil and Environmental Engineering, Florida International University, Miami, Florida 33174, USA

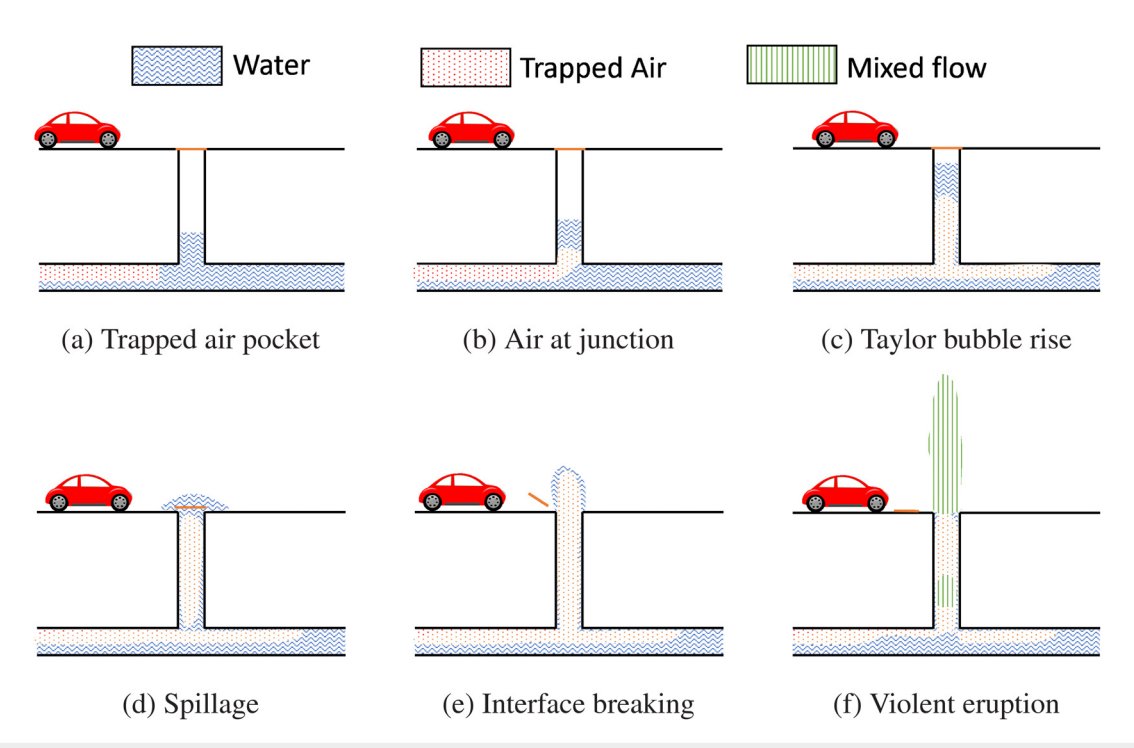


FIG. 1. Assumed stages of storm sewer geyser based on the current understanding.

enhanced with various experimentation and simulations. However, the replication of violent eruptions has not been widely reported in the open literature. In this work, a geyser is produced in a large-scale setup with sufficiently large pipe lengths and custom-designed water tanks. The large trapped air pockets are introduced through a pressurized air tank. This study primarily focuses on the occurrence of violent eruptions due to the air pocket size and operating conditions. The air pocket size is increased by increasing the air tank's initial pressure. This study identifies an abrupt transition of geyser characteristics with the increase in air pocket size. Also, the findings indicate the geyser severity transition depends on the operating conditions, i.e., the initial water pressure and velocity at the junction.

The remainder of the paper is structured as follows. First, a brief discussion on the current state-of-the-art focusing mainly on the experimental studies is provided. Second, a detailed methodology of the experiments where geometric details, measurement techniques, experimental procedures, and post-processing techniques are discussed. In the post-processing technique, a geyser score is introduced, which quantifies the eruption nature based on visual observations. Third, the experimental observations are discussed in three parts: (1) maximum geyser height, (2) effect of volume ratio, and (3) the effect of coefficient of pressure.

II. CURRENT STATE-OF-THE-ART

Researchers have been working on storm sewer geysers from the past four decades. The earliest study was conducted by Guo and Song⁵ to understand the role of pressure surging in geysers. However, this study concluded that the surging phenomenon does not produce violent geysers as seen in Minnesota. Wright *et al.*⁶ studied field data of storm sewer geysers and reported that the hydrostatic pressure head is

just 3 m in the 28 m long dropshaft. The pressure measurement did not show surging during the geyser event. After these findings, the hypothesis of the role of a trapped air pocket in producing violent geysers was widely explored. Muller et~al. Studied experimentally the role of fixed air pockets in producing geysers in a 0.305 m diameter PVC (polyvinyl chloride) pipe of 10.7 m length. The experimental observation showed spillage and small geyser eruptions. Since the initial pressure in the air pocket is kept similar to water pressure which resulted in the low volume ratio (\leq 0.25), violent eruptions were not observed. Figure 2 shows the concept of a trapped air pocket near the T-junction. The dimensions shown are used to calculate the volume ratio. The increase in air pocket size would result in a larger volume ratio. If the air is released from a pressurized tank, then the expected volume ratio can be high.

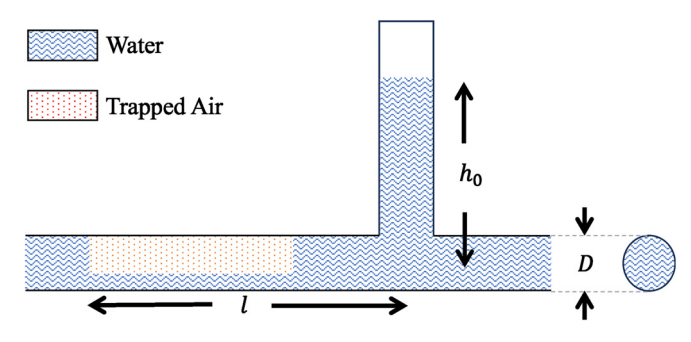


FIG. 2. Calculation of volume ratio which is the ratio of air pocket volume to the pipe volume of length $(I+h_0)$. I is the distance from the trailing edge of the air pocket to the junction, and h_0 is the pressure head at the junction.

Leon et al. went further with the trapped air pocket concept and experimentally investigated a large-scale geyser using an air tank of volume $1.7\,\mathrm{m}^3$. The air tank was pressurized to an elevated pressure, which resulted in a higher volume ratio. The large tank allowed an initial air-to-water volume ratio in the range of 4.5 to 7.8. The setup was able to generate violent geyser eruptions. The experiments showed the important mechanisms of geysers and the role of slugs in the eruptions. This study also demonstrated the requirement of a higher airwater volume ratio for violent geysers. However, the setup had a small pipe length ($<6\,\mathrm{m}$) between the drop shaft and the air tank and also utilized a fixed quantity of water which resulted in a system pressure drop with each eruption.

It is believed that the large air pocket formation is due to the rapid transition of gravity flow to the pressurized flow. The trapped air pocket size can depend on many parameters such as flow rate, initial water level, and various tunnel geometric parameters. The exact flow physics behind the large air pocket formation in the sewer tunnel is not clear and requires more research. However, some laboratory experiments have identified that the trapped air pocket size is correlated with the steepness of the water transient flow rate curve, and the inadequate ventilation can play a key role in air entrapment. Liu et al. 11 investigated a geyser generated by a sudden increase in the flow rate. The setup used a pair of partially open tailgate valves to trap large air pockets. The air pocket was set free and subjected to a large flow rate, which pushed it to the dropshaft. The interaction of air pockets with dropshaft was able to produce geysers. Using the same setup, Qian et al.¹² explored geyser mitigation techniques, such as recirculation chambers, benching, and orifice plates. This study concludes that mitigating geyser through a large flow resistance such as an orifice plate can result in very high peak pressure, whereas methods such as a recirculation chamber allow smoother air release with reduced geyser intensity. The use of a flow restrictor at the top of the junction also helps in geyser mitigation; however, a large volume of air is transported downstream, which may cause geyser at the next junction.

Li *et al.*¹³ numerically studied geysers using a trapped air pocket with both upstream and downstream treated as pressure boundaries. Zanje *et al.*¹⁴ demonstrated a numerical procedure for producing geysers using a fixed air inlet pressure where some of the important geyser characteristics such as Taylor bubble rise, low-intensity geyser, and

slug generations are observed. Slugs here refer to the liquid holdup in a stratified flow due to a large local gas velocity with respect to the liquid. The difference in velocity produces Kelvin–Helmholtz instabilities, which leads to the gas–liquid interface touching the pipe wall. Mahyawansi *et al.* 16 experimentally and numerically investigated small-scale geysers in a 0.025 m diameter PVC pipe, which captured important geyser stages such as Taylor bubble rise, slugs formation, and eruptions. The slug velocity measured by PIV (particle image velocimetry) was found around 0.9 m s $^{-1}$.

Large numbers of geyser experiments have been reported, but very few have shown violent geyser eruptions. Also, the previous experimental setups have had smaller scales in terms of pipe length and air-tank volume. The conventional water tanks used in previous experiments could not possibly maintain the fixed pressure boundaries, i.e., the water level in the tanks was not constant during geyser experiments. Additionally, the role of the air pocket volume for various operating conditions is yet to be thoroughly investigated. In the current study, the major upgrades in the experimental setup are a larger pipe length, larger air-tank volume, and custom-designed water tanks to maintain the fixed water level. The experimental study mainly focuses on the role of air volume ratio and operating conditions on the geyser intensity and maximum eruption height.

III. METHODOLOGY

The large-scale geyser experimental facility at Florida International University was constructed on an $18.2 \times 6\,\mathrm{m}$ concrete platform. Figure 3 shows the described experimental facility. The long 90° elbows were used to reduce separations and losses. Two custom-designed metal tanks with sliding gates were used to maintain the desired water level and to maintain the pressure boundary. The sliding gates allowed water heads in the range of $2.5-5\,\mathrm{m}$, which corresponded to $7.65\,\mathrm{to}\,15.28\,\mathrm{m}^3$ tank volumes. Dynatorque BG multiturn bevelgear drive mechanisms, powered by high-torque DC motors, were used to move the sliding gates. The water overflow from the sliding gates was collected in an overflow chamber. This water overflow from the sliding gates represented the constant pressure head. Both of the overflow chambers were connected to the four reserve tanks (black tanks shown in Fig. 3) of $4.0125\,\mathrm{m}^2$ capacity each via a $0.2032\,\mathrm{m}$ diameter polyvinyl chloride (PVC) pipe. The reserve tanks supplied water



FIG. 3. Experimental facility at the Florida International University.

to the $5600\,\mathrm{W}$ centrifugal pump, which delivered water to the main tank via a $0.0762\,\mathrm{m}$ diameter PVC pipe. The pump's maximum flow rate was $0.03\,\mathrm{m}^3\,\mathrm{s}^{-1}$ (440 gallons per minute) at $12\,\mathrm{m}$ height. The large pumping capacity allowed for a larger head difference in the experiment.

The diameter of the main tank's outlet was 0.2032 m, and it was connected to the gate valve. A 0.1572 m diameter PVC pipe was connected to the gate valve outlet using the eccentric reducer. At a region of interest, clear PVC pipes were used to visualize the air pocket movement. The remainder of the piping system was constructed using Schedule 80, 0.1572 m diameter PVC pipes and fittings. The detailed design and graphics were documented by Zanje *et al.*¹⁷

The pipes network is coiled using long 90° elbows to accommodate $88 \,\mathrm{m}$ long pipe system on an $18.2 \,\mathrm{m}$ long platform. A simplified schematic of the setup is shown in Fig. 4 with a coordinate system. Here, the coordinate x is along the horizontal pipe length. This helps in locating all the equipment and stations along the horizontal pipe. An air tank of $4.0125 \,\mathrm{m}^3$ was connected via a T-junction to the main line at $x = 44 \,\mathrm{m}$. A motorized butterfly valve was connected between the tank and the T-junction to remotely control the air insertion. The air tank was also connected to the two reciprocating compressors for air pressurization. The compressors and air tanks were connected via a solenoid valve to remotely cut off the compressors after attaining the desired air pressure. A check valve was placed just before the downstream tank to avoid flow reversal. The usage of the check valve was justified below.

The sudden drop in pressure due to geyser eruption is analogous to events such as closing a valve, which results in a sudden drop in velocity. This event creates a pressure wave in both upstream and downstream directions. The flow behind the wave will be brought to rest immediately, whereas the flow ahead of the wave will continue to have initial velocity. If l_d is the distance between the downstream end and the T-junction, and the pressure wave shall take l_d/a time to reach the downstream end, where a is the local speed of sound. The pressure

wave reflects back and returns at the same speed. Now, the flow behind the pressure wave is reversed, and the flow ahead of the wave is stagnant. Therefore, the pressure wave takes a total time of $2 \times l_d/a$ to return to the T-junction. The pressure wave moves with the local speed of sound a, which is approximately $1100 \, \mathrm{m \, s^{-1}}$ for pure water in the underground sewer tunnel pipes. The presence of large air pockets can reduce the speed of sound significantly due to an increase in the compressibility. Therefore, considering the actual tunnel system which is of several kilometers, the approximate time for the flow to reverse in the downstream vicinity of the T-junction can be of the order of minutes. This response time is called the communication time of the sewer tunnel. In the current experimental setup, the length of the downstream pipe is 23 m, which is too small to realize the required communication time. Hence, a check valve is used to prevent the reverse flow.

A. Measurement techniques

All the geyser experiments are monitored using six pressure sensors (GE UNIK 5000 series), one ultrasonic flow meter, and one camera. Figure 4 shows the position of the equipment and instrumentation. All the instruments except the video camera were connected to the National Instruments Data Acquisition (NI-DAQ 6321) system. The pressure sensors convert pressure into a voltage signal and were, therefore, calibrated using a liquid-filled industrial pressure gauge. The calibration was verified by changing the water head in stagnant conditions. The ultrasonic flow meter (Omega FDT-40) was programed for water in a 0.1572 m diameter PVC pipe, and it transmits measurements as a current signal. The flow meter separately displays the flow rate, which was used in the calibration of the current signals to the flow measurement. The NI-DAQ system records pressure, flow, and time at a 50 Hz sampling frequency in the continuous mode. The sampling rate was chosen to avoid a large buffer time that may result in large voids in the data. The sampling rate was chosen by trial and error.

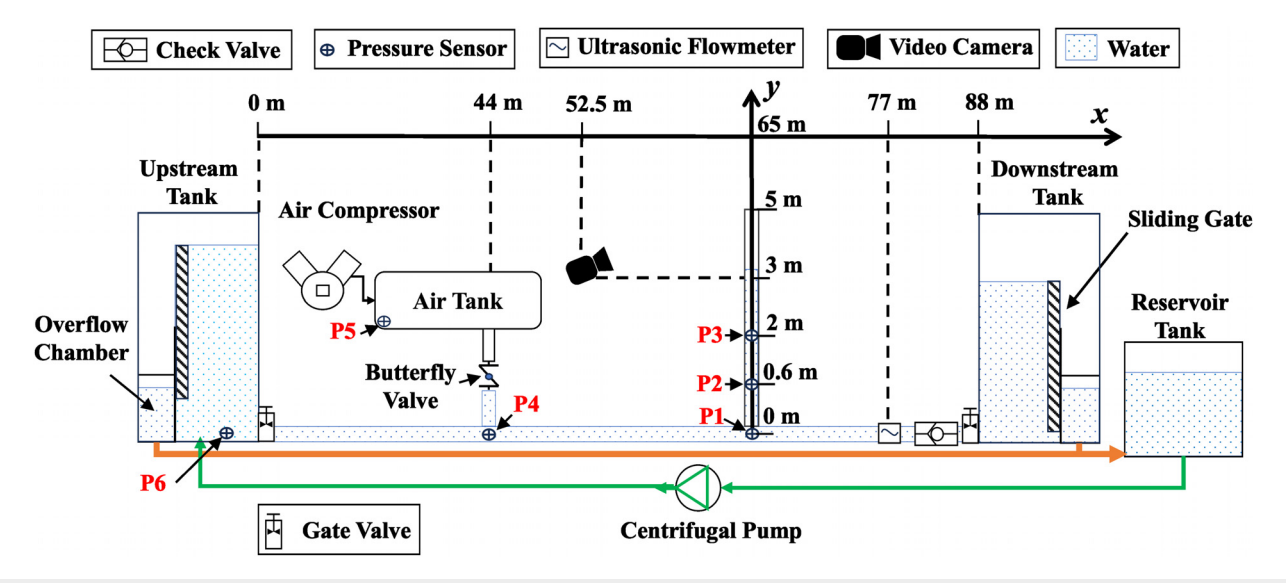


FIG. 4. Schematics of the geyser facility. The labels P1, P2, P3, P4, P5, and P6 are the pressure sensors. The length of the horizontal and the vertical pipe is 88 and 5 m, respectively.

A WiFi video camera (GMK wireless outdoor) of resolution 1920 \times 1080 was fixed in portrait orientation at 3 m above the ground and 12.1 m away from the vertical pipe. The camera imprints a time stamp on each frame, which helps in locating the frame on the temporal axis when compared with the NI-DAQ measurements. The pixel-to-distance relation was found using a large 4.5 m long steel pipe with a marking at the interval of 0.3048 m (1 ft). The rod is positioned at the top of the drop shaft to capture the region of interest. Each pixel corresponds to approximately 0.01 m along the vertical axis.

B. Experimental procedure

The steps for operating the large-scale geyser facility with a fixed quantity of air are shown below. The air tank was pressurized to a desired pressure, and then the compressors were disconnected using a solenoid valve, so that the experiment was performed with a fixed air mass.

- 1. Record the current local atmospheric pressure and temperature from an online weather report.
- 2. Adjust the sliding gate position of both the tanks to the desired position using the high-torque DC motor control.
- 3. Turn on the centrifugal pump to fill the water tanks and turn on the compressors. The compressor shuts down automatically upon reaching 90 psi.
- Turn on the DAQ reading for the steady flow operations (only water flow).
- 5. Once both the tanks are overflowing, monitor the pressure head at sensor P1 and the flow rate.
- Adjust the downstream sliding gate to achieve the desired velocity and pressure head.
- 7. Allow the system to reach a steady state (initial condition) and repeat the above step, if necessary.
- 8. Turn on the solenoid valve to pressurize the air tank.
- 9. Monitor the sensor P5 for the desired pressure and turn off the solenoid valve to cut off the air supply.
- Release air through another solenoid valve in case of an overpressurized tank.
- Verify all the variables, water velocity, pressure head, and air pressure.
- 12. Restart the DAQ reading for the transient operation and turn on the video recording.
- 13. Electrically trigger the butterfly valve to ON position, which opens smoothly and allows pressurized air to enter the horizontal pipe.
- 14. Observe and document the geyser eruptions.
- 15. After the release of all the major air pockets through the vertical pipe, the system will reach back to the initial conditions.
- 16. Turn off the butterfly valve position to OFF.
- 17. The air tank is now partially filled with water due to a large drop in air pressure. Hence, a drain valve is opened to release the water.

The fully instrumented geyser facility allows rapid testing of the cases with each case taking about approximately 10 to 12 min.

C. Post processing

The NI-DAQ stores data in a spreadsheet for a given case. A Python script was used to post-process the sensor data where the highfrequency pressure signal was filtered by a low-pass filter using the Scipy signal module.²² The FFT (fast Fourier transformation) of the measured pressure signals demonstrates that a frequency lower than 20 Hz covers the important geyser dynamics. This is also shown by Sumit *et al.*²³ using the numerical simulations.

The eruption pattern is studied using the video frames where all the frames are extracted as images in Python. The given image was subtracted using the previous image, and the edges of the difference image were extracted using the OpenCV module. The location of the highest edge in a given bound was considered as eruption height. The eruption height was calculated from the top of the vertical pipe. The algorithm's efficacy is demonstrated in Fig. 5(a) (Multimedia view). This automated image processing was used for selected cases where the background was relatively clear. The progression of geyser eruption height for these cases is discussed in Sec. IV. In most cases, the maximum height of the entire geyser process is manually reported from the video. Each geyser video was imprinted with a measurement scale using the pixel-to-distance relation value as shown in Fig. 5.

The air pocket's volume (V_a) in the horizontal pipe is estimated assuming the adiabatic expansion as shown in the following equation:

$$V_a = V_t \left(\frac{p_{ta}}{p_{ha}}\right)^{\frac{1}{\gamma}} - V_t, \tag{1}$$

where V_t is the air-tank volume (4.0125 m³), p_{ta} is the absolute air-tank pressure, p_{ha} is the initial absolute water pressure in the horizontal pipe at the air insertion location (measured by P4), and γ is the specific heat ratio for air and its value is 1.4.

The estimated air pocket's volume (V_a) is now used to define the volume ratio (V_R) , which is the ratio of air volume to the water volume as shown in the following equation:





(a) 0.1

(b) 0.1

FIG. 5. Example of geyser videos used for eruption height measurement. (a) shows the eruption peak detected using image processing, and (b) shows scales imprinted on the eruption videos to measure the maximum height. Multimedia available online.

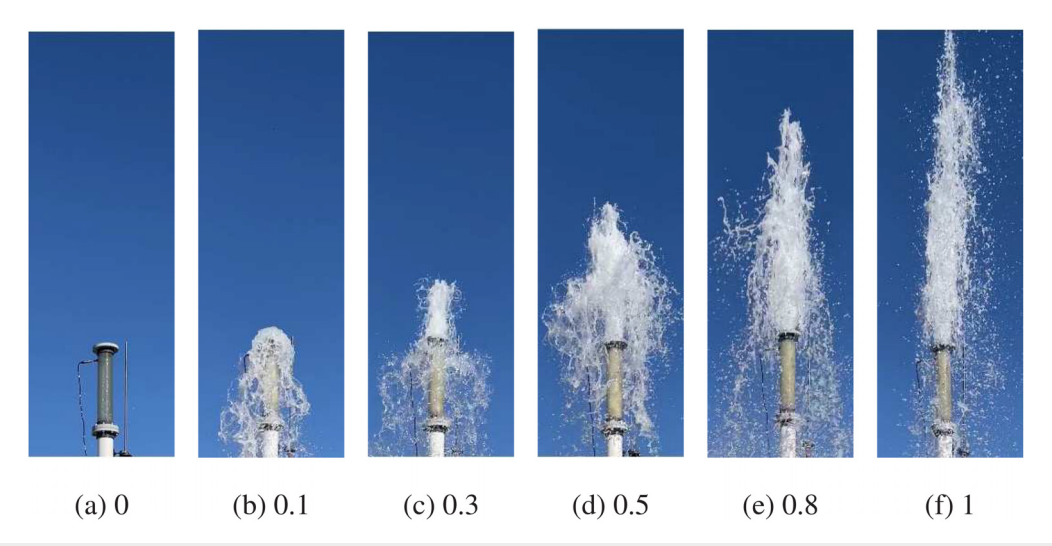


FIG. 6. Example of geyser score assignment: (a), (b), (c), (d), (e), and (f) represent the absence of a geyser, spillage, a small geyser, a medium-sized geyser, a well-developed geyser, and a violent geyser, respectively. The corresponding geyser scores are 0, 0.1, 0.3, 0.5, 0.8, and 1.

$$V_r = \frac{V_a}{V_w}. (2)$$

The water volume is calculated using the following equation:

$$V_{w} = (l + h_{0}) \cdot \frac{1}{4} \pi D^{2}, \tag{3}$$

where l is the distance between the air insertion junction and dropshaft junction, h_0 is the initial water head at the junction, and D is the pipe diameter. The volume ratio aids in quantifying the role of air in geyser occurrence.

The role of hydrostatic pressure and dynamic pressure can be combined using the coefficient of pressure (C_P),

$$C_P = \frac{p_{atm} + p_0}{\rho_w u_0^2}. (4)$$

Equation (4) shows the formula for calculating C_P , where p_{atm} is the atmospheric pressure, p_0 is the initial gauge pressure in the pipe at the junction, ρ_w is the standard water density (998.2 kg m⁻³), and u_0 is the initial average flow velocity in the horizontal pipe. C_P is the coefficient that multiplies by the pressure gradient term after non-dimensionalizing the momentum equation as shown by Mahyawansi *et al.*²⁵ In the case of the hypothesized situation of a geyser generated through a rapid filling, the pressure and velocity required for estimating C_P can be calculated from the initial and expected final flow properties after the geyser. This will be investigated in the future study. The role of C_P is discussed in detail in Sec. IV.

A geyser score parameter is introduced to quantify the severity of the geyser. This is based on the visual observation recorded during the experiments. The geyser score is slightly different than the maximum height, as it also identifies if the eruptions seem violent or simply spillage. For some operating conditions, the maximum eruption height may not be very high; however, they can be violent. Hence, a score is assigned based on the nature of the eruption observed. Figure 6 demonstrates the score assignment based on the shape and visible mixture profile. For spillage and small eruption, the score is 0.1 and 0.3, respectively. For geysers with good mixing and more lateral distribution of the mixture, a value of 0.5 is assigned. The geyser with visibly good

height and mixture distributed in the longitudinal direction is assigned 0.8. This is a critical stage, after which, if more air is available, the geyser will most likely transform into a violent one. The violent geyser will have a large velocity with highly atomized flow, which results in a cloud of fine droplets near the eruption peak.

D. Design of experiments

The experiments are conducted by varying the volume ratio from 0 to 1.1 for various operating conditions to investigate its effect on the geyser characteristics. The C_P is varied in the range of 500–2500. A total 116 cases are tested to study the effect of operating conditions and volume ratio on the violent geyser probability. The spreadsheet shared in the supplementary material shows the necessary details of the experiments conducted.

Figure 7 shows the distribution of volume ratio in the entire dataset. At least five tests are conducted for a given bin of volume ratio.

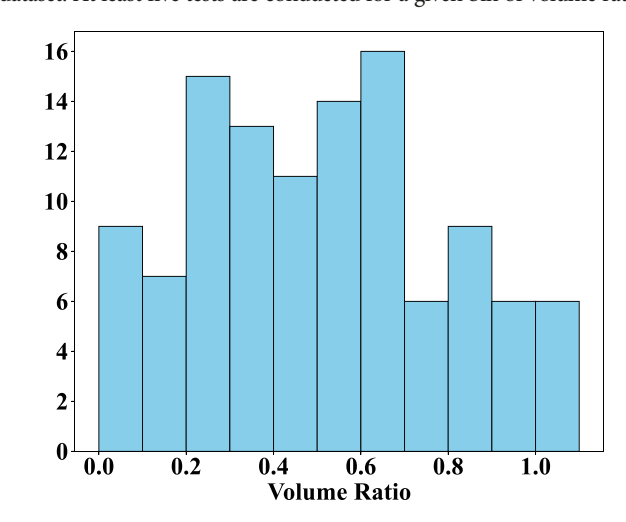


FIG. 7. Histogram of volume ratio (V_R) using a bin width of 0.1

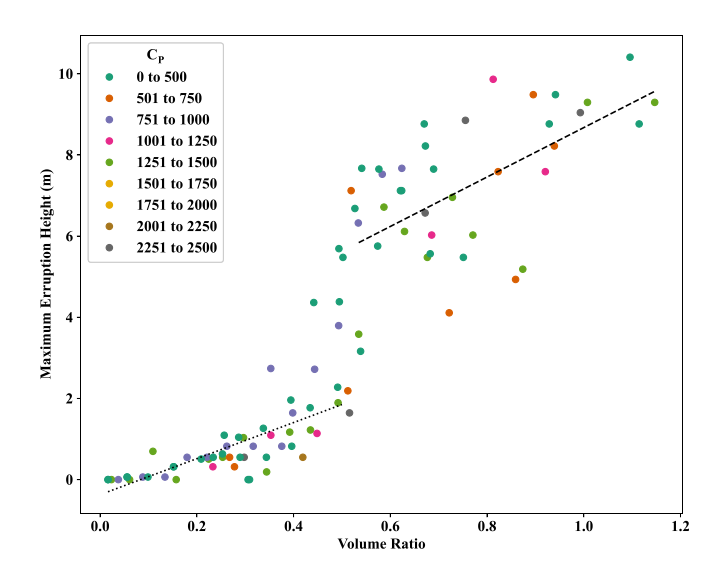


FIG. 8. Maximum eruption height for all cases. The markers are colored by C_P ranges.

The histogram peaks near a volume ratio 0.6 having more than 15 test cases. For the given operating conditions, the air-tank pressure is increased step by step, which results in a smoothly distributed volume ratio.

IV. RESULTS AND DISCUSSION

The experimental observation and results are described as follows. First, the trend of maximum geyser height for all the 116 cases is presented, and discontinuity in the trend is discussed. Second, the effect of volume ratio is discussed where the volume ratio is increased from 0 to 1.1 for 20 selected cases for the same initial water pressure and velocity. Third, the effect of C_P on the violent geysers is presented in which a linear relationship between volume ratio and C_P is found for a critical geyser score (0.8).

A. Maximum eruption height

One of the most important features of geysers is their eruption peak height. The magnitude of this height is a good measure of the severity of these eruptions. Figure 8 shows the trend of maximum height with the volume ratio. The markers are colored by the C_P . For all the cases, as the volume ratio approaches 0.5 from the left side, the eruption height increases almost linearly. The best-fit linear profile is shown as a dotted line. These are spillage or low-intensity geysers with poorly atomized interfaces. As the volume ratio reaches 0.5, a sharp increase in the geyser intensity is observed. This high-intensity geyser will have violent eruptions with a height greater than 5 m. Further increases in volume ratio result in a linear increment of eruption height up to 10 m. The best-fit linear profile is shown as a dashed line. The violent eruptions have a well-atomized air-liquid interface, i.e., a good air-water mixture is observed. However, one can speculate that the maximum height may get saturated as the volume ratio reaches some higher value because further diluted air-water mixtures lose momentum at a higher rate. This needs further investigation in the

The transition of geyser intensity at $V_R \simeq 0.5$ is demarking the air and water region of supremacy. In the water supremacy region

TABLE I. The twenty selected cases where air-tank pressure is increased step by step are presented. h_t is the gauge air-tank pressure. The initial flow condition is fixed at $h_0 = 3.584$ mH₂O and $u_0 = 0.295$ m s⁻¹.

Case	$h_t (\mathrm{mH_2O})$	V_R	High level observations	Geyser score	p_{atm} (Pa)
R1	3.618	0.02	Air-pockets in the dropshaft	0	101 617.86
R2	3.71	0.06	Large air-pockets in the dropshaft	0	101 611.54
R3	3.81	0.11	Spillage	0.1	101 603.64
R4	3.91	0.16	Mixed flow in dropshaft	0	101 598.1
R5	4.05	0.22	Mixed flow spillage	0.1	101 592.57
R6	4.11	0.25	Mixed flow spillage	0.1	101 588.62
R7	4.2	0.30	Small height geyser	0.3	101 583.09
R8	4.3	0.34	Mixed flow spillage	0.1	101 578.35
R9	4.4	0.39	Small height geyser	0.3	101 570.45
R10	4.49	0.44	Small height geyser	0.3	101 558.6
R11	4.61	0.49	Medium height geyser	0.5	101 553.07
R12	4.7	0.53	Good height geyser	0.8	101 541.21
R13	4.81	0.59	Violent geyser	1	101 534.1
R14	4.9	0.63	Violent geyser	1	101 528.57
R15	5	0.68	Violent geyser	1	101 523.83
R16	5.11	0.73	Violent geyser	1	101 515.14
R17	5.2	0.77	Violent geyser	1	101 508.82
R18	5.42	0.87	Violent geyser	1	101 502.5
R19	5.71	1.01	Violent geyser	1	101 723.74
R20	6.01	1.15	Violent geyser	1	101 723.74

 $(V_R < 0.5)$, the primary mechanism of the geyser is buoyancy. The air pocket in the horizontal pipe smoothly breaks at the junction due to Rayleigh–Taylor instability and produces smaller air pockets in the vertical pipe. The smooth process of air pocket production allows the system to maintain the pressure equilibrium, and, hence, pressure spikes are not observed. This produces spillage and small geysers if the water level in the dropshaft is initially high.

In the air supremacy region ($V_R > 0.5$), the size of the air pocket in the horizontal pipe stays intact for a longer time and supplies air at higher flow rates. This results in a higher Weber number and a finely atomized interface. The multi-point breaking of the interface produces a good mixture, which results in the production of a series of air pocket trails by a highly atomized flow. The first air pocket in the vertical pipe spills the water to expose the entire column to the ambient pressure. This results in the dropshaft depressurization. The depressurization further increases the air flow rate and accelerates the mixture to a high upward velocity. The large pressure drop shows the rapid acceleration

of the mixture and violent eruptions. The high air velocity in the horizontal pipe produces slugs, which can also contain a finely atomized mixture and result in subsequent violent eruptions. These eruptions due to mixed slugs are the most violent and achieve the maximum height. This can be seen in some cases in Fig. 10 where the second peak is the highest. This will be further investigated in future studies.

The magnitude of C_P plays an important role in the transition of the small geyser to the violent geysers. The lower C_P cases appear to get violent at a lower volume ratio of around 0.4. This is further discussed in Sec. IV C. Interestingly, the scatter in data points for lower C_P values is higher, and it gets further spread for higher volume ratio. This is probably because the lower C_P values have a higher Reynolds number and, hence, have significant turbulence influence. Additionally, in the violent eruptions zone, the complex interfacial dynamics may further increase the turbulent intensity, and, hence, a larger scatter is observed. This needs further investigation through data analysis and numerical simulations in the future.

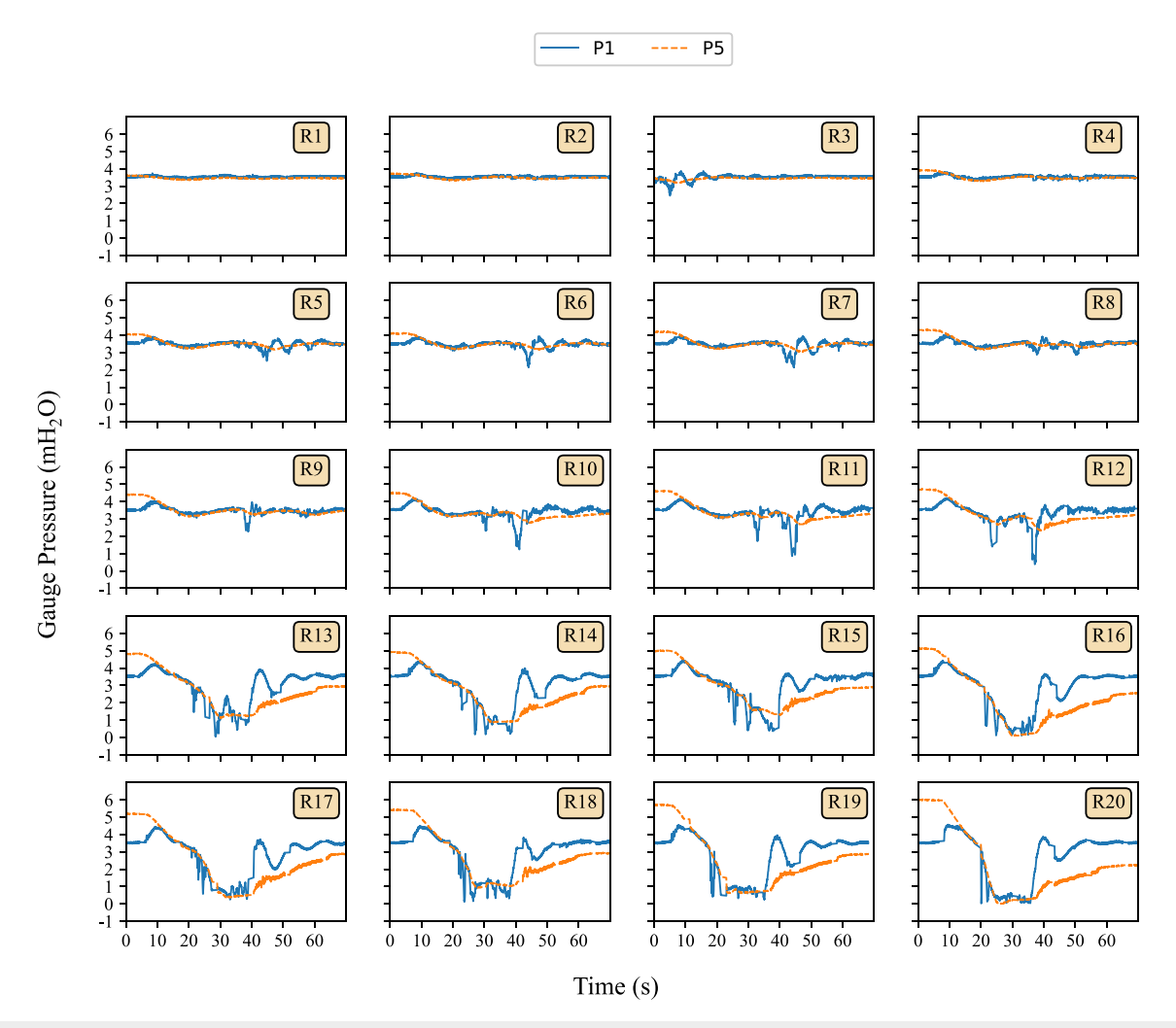


FIG. 9. Pressure temporal history for cases R1–R20 measured by sensors P1 and P5

B. Effect of volume ratio

To understand the effect of volume ratios, 20 cases are selected from the dataset where the initial flow parameters are kept constant. Table I shows the selected cases where the air-tank pressure is increased gradually to increase the volume ratio (V_R) .

Figure 9 shows the static pressure variation at sensors P1 and P5 for cases R1-R20. Correspondingly, Fig. 10 (Multimedia view) shows the eruption height with the relative time. For cases from R1 to R8, minor perturbation in the pressure is observed, which is due to the smaller size of air pockets. In these cases, the air pockets simply produce spillage, and the duration of the spillage increases as volume ratio increases. There is an exception noted where case R3 produces spillage and case R4 does not. This is because case R4 is the first case where the air pocket gets atomized and forms a uniform mixture that rises but does not spill. The following cases R5 and R6 with slightly larger air pockets are able to produce spillage of mixed flow as mentioned in Table I. From cases R9-R12, small geysers to medium-sized geysers are observed, which have multiple eruptions in a pattern where the eruption height increases gradually and then decreases. The corresponding pressure measurement for these cases shows one or two major pressure drop incidents. In each incident, the pressure drops in multiple oscillatory steps instead of one smooth monotonous curve.

The gradual drop in pressure with each step shows a gradual increase in eruption height.

Cases from R13 to R18 show the continuous pressure drop, which encompasses a few large magnitude sharp drops. Each of these large sharp drops represents one eruption. In each case, one or two violent eruptions are observed, which can reach up to 9 m from the pipe outlet. The number of eruptions increases from R13 to R18 with maximum eruption height remaining almost constant. In this case, the geyser height gradually increases with subsequent eruption till it reaches a maximum after which it steeply decreases. Depending on the volume ratio, one or two eruptions are observed at the maximum height. For cases R19 and R20, the large volume ratio results in further high eruption height, and a large number of eruptions in a short time are observed. In these cases, all the water in the horizontal pipe is rapidly used up in producing violent eruptions, resulting in the sole presence of air in the horizontal pipe. Once the air pressure drops, water fills the system again, as seen in the pressure drop.

The air-tank pressure (P5) drops in accordance with the sensor P1, which is at the main junction. This shows the main junction leads the geyser process, and violent eruptions can result in a sharp pressure drop in the horizontal and vertical pipes, which drains the air-tank to almost negative gauge pressure.

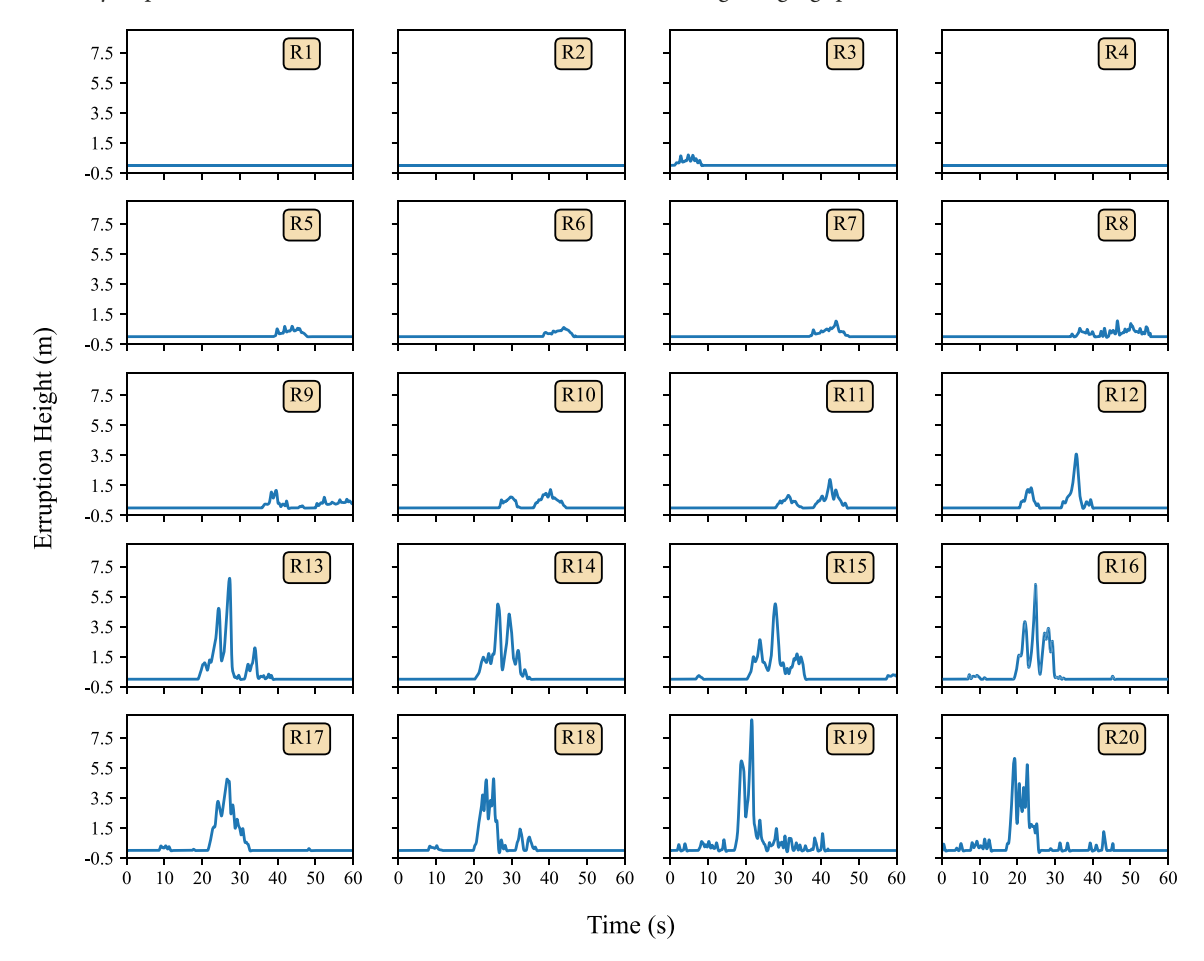


FIG. 10. Eruption temporal history for cases R1-R20 calculated from videos. Multimedia available online.

C. Effect of Cp

The coefficient of pressure (C_P) affects the slug's length and mixing.²⁵ Higher C_P values favor the production of a large number of small slugs, whereas lower values can produce a small number of large slugs. Additionally, the slugs produced at lower C_P grow and atomize in their path, resulting in a large, fast-moving slug with entrained air—a favorable recipe for a violent eruption.

Figure 11 shows the plot of volume ratio and C_P . The markers are colored by the geyser score and sized by the operating pressure head. A geyser score of 0.8 represents eruptions that appear to be transitioning from low-intensity geysers to high-intensity geysers. The trace of this geyser score is shown by the linearly best-fitted dashed line (say the critical line). The critical line has a positive slope, indicating that a higher C_P requires a higher volume ratio to generate violent geysers. Since the sample points are not uniform and sufficient in C_P space, this observation may vary with different sets of experiments, and, hence, more experiments are required.

All the violent geyser cases near the critical line have an eruption progression from a small height to a violent eruption. This development of eruptions is entirely due to the large air pocket inside the horizontal pipe, which initially spills water from the vertical pipe and gradually depressurizes it. The pressurized air pocket rushes to the vertical pipe, producing slugs. For a low C_P value, these slugs are large in size and contain a good amount of air–water mixture. These fastmoving slugs enter the vertical pipe and shoot upward at high speed, producing violent eruptions. For higher C_P values, the slug is smaller in size and contains a lean air–water mixture for the same volume ratio, and, hence, its eruptions are less violent.

D. Key findings

The geyser experiments with a fixed air mass showed two major findings: first, the geyser intensity transitions from a small height geyser to a violent one as the air—water volume ratio increases, and second, the minimum volume ratio required for a violent eruption linearly increases with the coefficient of pressure. This can be

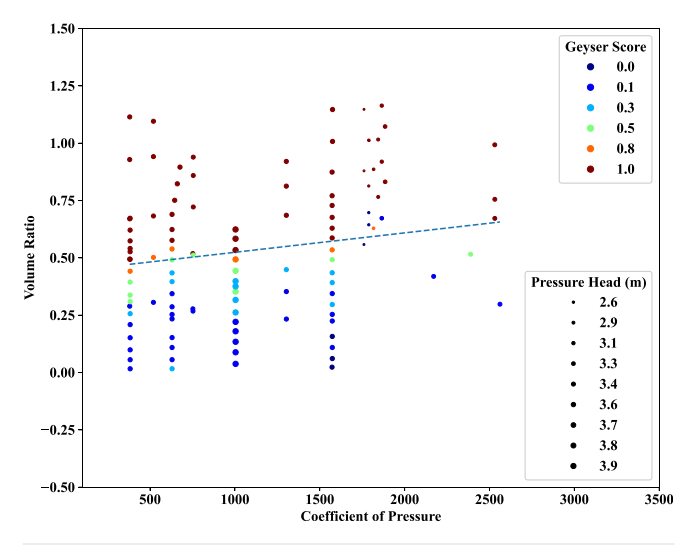


FIG. 11. Effect of C_P on the occurrence of geyser. The markers are colored and sized according to the geyser score and the pressure head, respectively.

interpreted for an actual storm sewer geyser, where the large air pocket that forms in the event of rapid filling may have a higher chance of a violent geyser if it is formed closer to the vertical pipe or is able to convect without stretching, satisfying $V_R \geq 0.5$.

The required air pocket size reduces if C_P is lower, i.e., with low operating pressure and high-pressure gradient. The low operating pressure results in a larger air pocket volume for a given air mass, and the high flow velocities force the air pocket downstream and compress it against the water, resulting in a larger air pocket volume per unit length of the pipe. This behavior of air pockets with operating conditions has been observed in a few experimental and numerical studies. 25,27

In the current study, the violent geyser lasts for 10 to 12 s in contrast to Leon's experimental study where it lasts for only 2 to 3 s.²⁶ This is mainly due to the current setup having a longer pipe length between the air tank and the vertical pipe compared to the previous studies. The longer pipe length allows large volumes of air pockets for similar volume ratios. However, in the actual storm sewer geyser, the eruptions last for tens of seconds, which is probably due to two reasons, first the large length of sewer tunnel can have a large air pocket of the order of 100 m in length, and second, the highly mixed eruption flow can have a speed of sound as low as $22 \,\mathrm{m \, s}^{-1,26,28}$ which may result in choked condition limiting the maximum eruption velocity and thereby limiting the maximum air release rate.²⁹ Therefore, large air volume and limited air release rate can result in long-lasting geysers. Based on this understanding, geyser mitigation strategies can be devised, which focus on the air ventilation system to avoid air entrapment and retrofit designs that allow the smooth release of trapped air.

In addition to these findings, the experimental measurement provides sufficient cases for validating the numerical simulation strategy to predict such a highly unsteady multiphase flow. The pressure plot and eruption height trend can be good metrics to test the fidelity of the numerical simulation.

V. CONCLUSIONS

A large-scale geyser experiment is conducted using a pressurized air tank. A total of 116 test cases are considered where an important parameter, volume ratio, is varied for different operating conditions. This study mainly discusses the pressure plots and eruption height measurements. This study quantifies the nature of geysers and eruptions using the geyser score, which is based on visual observations during the experiments. The geyser score ranges from 0 to 1, where 0 represents no geyser case and 1 represents a violent geyser. The eruption progression is measured using image processing techniques, which helped in understanding its relationship with pressure spikes.

The important observations are the geyser intensity and maximum eruption height increase with the volume ratio which at $V_R = 0.5$ experiences a sharp transition to violent geysers. The low volume ratio ($V_R < 0.5$) cases generate a spillage and a poorly atomized small-height geyser, and the height and number of eruptions increase with the volume ratio. The higher volume ratio cases ($V_R > 0.5$) generate violent geyser eruptions, which are identified by their high visible speed and height of eruptions. Additionally, the violent eruptions have a finely atomized mixture, which further improves with an increase in the volume ratio.

The maximum eruption height of violent geysers also increases linearly with the volume ratio up to the tested $V_R = 1.1$. However, it is uncertain whether the height will continue to increase linearly

indefinitely, a matter that will be investigated in the future. The operating condition is quantified by the coefficient of pressure (C_P). The critical volume ratio at which geyser intensity abruptly increases is linearly proportional to C_P . The scientific reason for this linear relationship will be investigated in the future.

SUPPLEMENTARY MATERIAL

See the supplementary material for the experimental details given as a spreadsheet of all 116 test cases mentioned in the article. The details include initial flow velocity and pressure head, initial air-tank pressure, high-level observations, geyser scores, volume ratio (V_R), and coefficient of pressure (C_P).

ACKNOWLEDGMENTS

The authors would like to thank the late Professor Cheng-Xian Lin for his support and guidance in this work. The authors would also like to thank the support in the experimentation by Mr. Lucas Hurley, Mr. Jesus Galarza, and Mr. Michael Hidalgo.

The authors gratefully acknowledge the financial support of the National Science Foundation (NSF) under Grant No. 1928850. The views expressed are solely those of the authors. NSF does not endorse any products or commercial services mentioned.

AUTHOR DECLARATIONS Conflict of Interest

The authors have no conflicts to disclose.

Author Contributions

Pratik Mahyawansi: Conceptualization (lead); Data curation (lead); Formal analysis (lead); Investigation (lead); Methodology (equal); Software (lead); Validation (lead); Visualization (lead); Writing - original draft (lead); Writing - review & editing (equal). Sumit R. Zanje: Conceptualization (equal); Data curation (equal); Formal analysis (equal); Methodology (equal). Abbas Sharifi: Conceptualization (supporting); Data curation (equal); Formal analysis (equal); Investigation (equal); Methodology (equal); Validation (equal). Dwayne McDaniel: Conceptualization (equal); Project administration (equal); Resources (supporting); Supervision (equal); Validation (equal); Writing - review & editing (equal). Arturo S. Leon: Conceptualization (equal); Data curation (supporting); Formal analysis (equal); Funding acquisition (equal); Investigation (equal); Methodology (equal); Project administration (equal); Resources (equal); Software (equal); Supervision (equal); Validation (equal); Visualization (equal); Writing - review & editing (equal).

DATA AVAILABILITY

The data that support the findings of this study are available from the corresponding author upon reasonable request.

NOMENCLATURE

- a Speed of sound in water (m s⁻¹)
- C_p Coefficient of pressure
- D Pipe diameter (m)

- g Acceleration due to gravity ($m s^{-2}$)
- h_t Initial air-tank pressure head (mH₂O)
- h_0 Initial water head (m)
- Distance between the air injection point to the dropshaft
 (m)
- l_d Distance between dropshaft and downstream end (m)
- *p*_{atm} Atmospheric pressure (Pa)
- p_{ha} Absolute water pressure in pipe (Pa)
- p_{ta} Absolute air-tank pressure (Pa)
- p_{th} Gauge air-tank pressure (Pa)
- p_0 Initial gauge pressure (Pa)
- T Temperature (K)
- t Time (s)
- u_0 Initial average water velocity (m s⁻¹)
- V_a Estimated air pocket volume (m³)
- V_R Volume ratio
- V_w Total volume of water from the air-tank to the dropshaft including the water in the dropshaft (m³)
- x X-coordinate (m)
- y Y-coordinate (m)
- γ_1 Air specific heat ratio
- ρ_w Water density (kg m⁻³)

REFERENCES

- ¹E. M. Brandon, "How sewer geysers became the terrifying new environmental trope of the climate change era" (2022), see https://www.fastcompany.com/90793843/how-sewer-geysers-became-the-terrifying-new-environmental-trope-of-the-climate-change-era
- ²L. Henny, C. D. Thorncroft, and L. F. Bosart, "Changes in seasonal large-scale extreme precipitation in the mid-Atlantic and northeast United States, 1979–2019," J. Clim. 36, 1017–1042 (2023).
- ³S. Habel, C. H. Fletcher, T. R. Anderson, and P. R. Thompson, "Sea-level rise induced multi-mechanism flooding and contribution to urban infrastructure failure," Sci. Rep. 10, 3796 (2020).
- ⁴J. H. Nienhuis, W. Kim, G. A. Milne, M. Quock, A. B. Slangen, and T. E. Törnqvist, "River deltas and sea-level rise," Annu. Rev. Earth Planet. Sci. 51, 79–104 (2023).
- ⁵Q. Guo and C. C. Song, "Surging in urban storm drainage systems," J. Hydraul. Eng. 116, 1523–1537 (1990).
- ⁶S. J. Wright, J. W. Lewis, and J. G. Vasconcelos, "Physical processes resulting in geysers in rapidly filling storm-water tunnels," J. Irrig. Drain. Eng. 137, 199–202 (2011).
- ⁷K. Z. Muller, J. Wang, and J. G. Vasconcelos, "Water displacement in shafts and geysering created by uncontrolled air pocket releases," J. Hydraul. Eng. 143, 04017043 (2017).
- ⁸A. S. Leon, I. S. Elayeb, and Y. Tang, "An experimental study on violent geysers in vertical pipes," J. Hydraul. Res. 57, 283–294 (2019).
- ⁹L. Ramezani, B. Karney, and A. Malekpour, "Encouraging effective air management in water pipelines: A critical review," J. Water Resour. Plann. Manage. 142, 04016055 (2016).
- ¹⁰J. G. Vasconcelos and S. J. Wright, "Mechanisms for air pocket entrapment in stormwater storage tunnels," in World Environmental and Water Resource Congress: Examining the Confluence of Environmental and Water Concerns, 2006
- ¹¹L. Liu, W. Shao, and D. Z. Zhu, "Experimental study on stormwater geyser in vertical shaft above junction chamber," J. Hydraul. Eng. 146, 04019055 (2020).
- ¹²Y. Qian, D. Z. Zhu, L. Liu, W. Shao, S. Edwini-Bonsu, and F. Zhou, "Numerical and experimental study on mitigation of storm geysers in Edmonton, Alberta, Canada," J. Hydraul. Eng. 146, 04019069 (2020).
- ¹³X. Li, J. Zhang, D. Z. Zhu, and S. Qian, "Modeling geysers triggered by an air pocket migrating with running water in a pipeline," Phys. Fluids 35, 045126 (2023).

- ¹⁴S. R. Zanje, P. Mahyawansi, A. S. Leon, and C.-X. Lin, "CFD modeling of storm sewer geysers in partially filled dropshafts," in World Environmental and Water Resources Congress (ASCE, 2022), pp. 1187–1195.
- ¹⁵K. Mishima and M. Ishii, "Theoretical prediction of onset of horizontal slug flow," J. Fluids Eng. 102, 441–445 (1980).
- 16P. Mahyawansi, S. R. Zanje, A. Sharifi, D. McDaniel, and A. S. Leon, "Experimental and numerical investigation of a small scale storm sewer geyser," J. Hydraul. Res. 62, 25–38 (2024).
- 17 S. R. Zanje, P. Mahyawansi, A. Sharifi, A. Leon, V. Petrov, Y. Y. Infimovskiy et al., see https://ssrn.com/abstract=4710995 or http://dx.doi.org/10.2139/ssrn.4710995 for "Experimental study of sewer geysers in vertical shafts."
- ¹⁸Sulzer Pumps Ltd, "4—Special data for planning centrifugal pump installations," in *Centrifugal Pump Handbook*, edited by Sulzer Pumps Ltd. (Elsevier, Oxford, 1989), pp. 109–162.
- 19G. Z. Watters, "The behavior of PVC pipe under the action of water hammer pressure waves," Reports, Paper 20 (1971), see https://digitalcommons.usu.edu/ water_rep/20.
- ²⁰I. Pearsall, "Paper 2: The velocity of water hammer waves," in *Proceedings of the Institution of Mechanical Engineers, Conference Proceedings* (SAGE Publications/Sage UK, London, UK, 1965), Vol. 180, pp. 12–20.
- ²¹F. Zhou, F. Hicks, and P. Steffler, "Transient flow in a rapidly filling horizontal pipe containing trapped air," J. Hydraul. Eng. 128, 625–634 (2002).
 ²²P. Virtanen, R. Gommers, T. E. Oliphant, M. Haberland, T. Reddy, D.
- ²²P. Virtanen, R. Gommers, T. E. Oliphant, M. Haberland, T. Reddy, D. Cournapeau, E. Burovski, P. Peterson, W. Weckesser, J. Bright, S. J. van der

- Walt, M. Brett, J. Wilson, K. J. Millman, N. Mayorov, A. R. J. Nelson, E. Jones, R. Kern, E. Larson, C. J. Carey, İ. Polat, Y. Feng, E. W. Moore, J. VanderPlas, D. Laxalde, J. Perktold, R. Cimrman, I. Henriksen, E. A. Quintero, C. R. Harris, A. M. Archibald, A. H. Ribeiro, F. Pedregosa, P. van Mulbregt, and SciPy 1.0 Contributors, "SciPy 1.0: Fundamental algorithms for scientific computing in python," Nat. Methods 17, 261–272 (2020).
- python," Nat. Methods 17, 261–272 (2020).

 23 R. Z. Sumit, "Sewer geyser mechanism and mitigation strategies," Ph.D. thesis
 (Florida International University, Miami, FL, 2023).
- ²⁴G. Bradski, "The OpenCV Library," Dr. Dobb's J. Software Tools 120, 122–125 (2000).
- 25P. Mahyawansi, C.-X. Lin, and A. S. Leon, "Understanding the influence of pressure disturbance on the transition of stratified to slug flow," in 7th Thermal and Fluids Engineering Conference (TFEC), 2022.
- 26A. S. Leon, "Mechanisms that lead to violent geysers in vertical shafts," J. Hydraul. Res. 57, 295–306 (2019).
- ²⁷T. Liu and J. Yang, "Experimental studies of air pocket movement in a pressurized spillway conduit," J. Hydraul. Res. 51, 265–272 (2013).
- ²⁸K. Fu, X. Deng, L. Jiang, and P. Wang, "Direct numerical study of speed of sound in dispersed air-water two-phase flow," Wave Motion 98, 102616 (2020)
- ²⁹A. S. Leon, "Upper limit velocity of geyser eruptions in stormwater and combined sewer systems," in World Environmental and Water Resources Congress (American Society of Civil Engineers, Reston, VA, 2019), pp. 122-128.